Journal of Advances in Medical and Biomedical Research | ISSN:2676-6264

Co-culture-based three-dimensional culture platforms to enhance the *in vitro* survival and proliferation of U266 myeloma cells

Mohammadmahdi Khosravi [1], Sadaf Vahdat [2*], Saeid Abroun [1]

1. *Department of Hematology, Faculty of Medical Sciences, Tarbiat Modares University, Tehran, Iran*
2. *Applied Cell Sciences Division, Department of Hematology, Faculty of Medical Sciences, Tarbiat Modares University, Tehran, Iran*

Article Info

Received: 2026/01/13;

Accepted: 2026/04/12;

Published Online: 2026/06/29;

***Corresponding author:**

Sadaf Vahdat,

Applied Cell Sciences Division, Department of Hematology, Faculty of Medical Sciences, Tarbiat Modares University, Tehran, Iran

Email: s_vahdat@modares.ac.ir

How to Cite This Article:

Khosravi M, Vahdat S, Abroun S. Co-culture-based three-dimensional culture platforms to enhance the *in vitro* survival and proliferation of U266 myeloma cells. J Adv Med Biomed Res 2026; 34(3):251-260.

ABSTRACT

Background & Objective: It has been demonstrated that three-dimensional (3D) interactions among myeloma cells, other cellular components, and extracellular matrix (ECM) constitutes within the bone marrow (BM) microenvironment play critical roles in disease progression. Therefore, the *in vitro* recapitulation of interactions would advance the fields of disease modeling and drug screening. In this regard, we aimed to develop simple, cost-effective, and available 3D culture conditions for U266 cells using co-culture systems to more closely mimic their native microenvironment.

Materials & Methods: U266 cells, BM-derived mesenchymal stem cells (BM-MSCs) and human umbilical vein endothelial cells (HUVECs) were co-cultured in different matrix-based and matrix-free conditions. Subsequently, the viability and proliferation rates of U266 cells were evaluated and compared. Peripheral blood (PB) plasma was used to generate fibrin gels for matrix-based structures.

Results: Co-cultured cells in the gel-free group generated and assembled into 3D cell structures. Moreover, the viability and expansion fold of U266 cells in the gel-free group were significantly higher compared with those in the on-gel and inside-gel groups.

Conclusion: Our simple gel-free 3D co-culture system of U266 cells with BM-MSCs and HUVECs, which demonstrated higher viability and proliferation rates of myeloma cells, can serve as a platform for further *in vitro* studies, including drug screening.

Keywords: Multiple myeloma, Co-culture, Three-dimensional cell culture, Fibrin, Proliferation

1. Introduction

Despite the efforts made to introduce novel therapeutic approaches, multiple myeloma (MM), one of the most common hematological malignancies, is still incurable (1); this has attracted researchers to more precisely study the malignant microenvironment to figure out the disease pathogenesis (2). On the other hand, most preclinical studies could not successfully translate to clinics because of the lack of appropriate *in vitro* and *in vivo* myeloma disease models (3). It has been shown that direct and indirect interactions between malignant cells and other cell types in their microenvironment affect disease progression and drug resistance (4). The bone marrow (BM) microenvironment consists of various cell types, including hematopoietic stem cells, mesenchymal stromal cells (MSCs), endothelial cells, osteoblasts and osteoclasts. MM cells interact with BM mesenchymal stem cells (BM-MSCs), which induce NF-κB and IL-6 secretion by BM-MSCs. IL-6 promotes the survival of MM cells by activating proliferative and anti-apoptotic pathways (5). MM cells and BM-MSCs induce angiogenesis by secreting VEGF, bFGF and matrix metalloproteinase. VEGF can stimulate proliferation and chemotaxis in endothelial cells, and BM angiogenesis is considered an important factor in promoting MM progression (6). Therefore, the complex and dynamic three-dimensional (3D) interplays determine and regulate differentiation, migration, proliferation, survival, progression and drug resistance of MM cells (7), and accordingly, considering these interactions can lead to a more similar recapitulation of the myeloma microenvironment for disease study and drug screening (8).

Animal models offer advantages over two-dimensional (2D) cell cultures by recreating the complexity of the BM, but human and animal disease microenvironments and immunity vary significantly (9). Therefore, several

scaffold-based and scaffold-free human culture systems have been developed to overcome the limitations of animal models as well as 2D cell cultures for recapitulation of the heterogeneous MM microenvironment (10). Different types of matrices, including silk, Matrigel, acrylic polymers and hyaluronic acid, have been introduced to fabricate multiple myeloma 3D structures; however, most of them are not naturally found in the BM microenvironment(11). Fibrin gels derived from plasma samples are natural matrices suitable for the culture of myeloma primary cells and cell lines and have been used in several studies (12, 13). Moreover, various approaches have been developed to generate tissue-like 3D structures in matrix-free conditions (14). Matrix-free culture systems take advantage of cells' natural ability to self-aggregate without biomaterials and to secrete their own ECM components over time (15). It should be emphasized that all these *in vitro* structures can be generated by using patients' samples to recapitulate the disease microenvironment as closely as possible; however, the availability of patients' samples as well as the reproducibility of the generated structures are challenging issues (16). Accordingly, the generation of patient-independent culture systems using cell lines could advance the field of myeloma disease modeling due to their ease of handling, self-replication, availability and homogenous nature (17).

In this study, we aimed to develop simple, cost-effective, and accessible 3D myeloma structures without the need for patient-derived samples. To achieve this, U266 cells were co-cultured with BM-MSCs and human umbilical vein endothelial cells (HUVECs) under different culture conditions: peripheral blood (PB)-derived fibrin gel-based and gel-free systems. The culture systems were compared based on myeloma cell viability and proliferation rates.

2. Materials and Methods

2.1 Cell culture procedures

U266 cell line (human myeloma, IBRC C10148) was obtained from the Iranian National Center for Genetic and Biologic Resources. U266 cells were cultured in RPMI-1640 (Cat# 035-51800, Gibco, USA) complete culture medium containing 10% FBS (Cat# BI-1201, Bioidea, Tehran, Iran) and 1% penicillin/streptomycin (Cat# BI-1203, Bioidea, Tehran, Iran) at 37°C, 95% humidity, and 5% CO_2. The medium was changed every three days. Cells were subcultured at a density of 3×10^5 cells/ml.

BM-MSCs, (RSCB0787) were purchased from Royan Stem Cell Bank (RSCB), Royan Institute. Cells were cultured in low glucose DMEM (Cat# BI-1004, Bioidea, Tehran, Iran) supplemented with 10% FBS and 1% penicillin/streptomycin at 37°C, 5% CO_2 and 95% humidity. The medium was changed every three days. Cells were passaged upon reaching approximately 70-80% confluence using trypsin/EDTA 0.025% (Cat# BI-1602, Bioidea, Tehran, Iran) treatment and seeded at a density of 8×10^4 cells/cm^2. In order to assess the BM-MSCs differentiation potential into osteoblasts and adipocytes, BM-MSCs were cultured in osteogenic (Cat# BI-1102, Bioidea, Tehran, Iran) and adipogenic (Cat# BI-1101, Bioidea, Tehran, Iran) differentiation induction media for 21 and 14 days, respectively. Alizarin Red (Cat# BI-1801, Bioidea, Tehran, Iran) and Oil Red O (Cat# BI-1802, Bioidea, Tehran, Iran) staining protocols were used to evaluate osteogenic and adipogenic differentiation, respectively. Human umbilical vein endothelial cells, RSCB0780 were provided from Royan Royan Stem Cell Bank (RSCB), Royan Institute. HUVECs were cultured in EGM-2 (Cat# CC-3202, Lonza, USA) supplemented by 10% FBS and 1% penicillin/streptomycin at 37°C, 5% CO_2 and 95% humidity. The medium was changed every three days. Cells were passaged upon reaching approximately 70-80% confluence using trypsin/EDTA treatment and seeded at a density of 1×10^5 cells/cm^2.

2.2 Flow cytometry analysis

The expression of CD138 on U266 cells, CD31 on HUVECs, and CD90 and CD105 on BM-MSCs was assessed by flow cytometry. Single cells were washed with PBS (Cat# BI-1401, Bioidea, Tehran, Iran) and thereafter resuspended at a density of 10^5 cells in 100 µl PBS. They were incubated with conjugated antibodies, FITC-conjugated CD138 (Cat# IQP-153F, IQ Products, Netherlands), PE-conjugated CD31 (Cat# 303105, BioLegend, USA), APC-conjugated CD90 (Cat# 328113, BioLegend, USA) and PE-conjugated CD105 (Cat# 323205, BioLegend, USA), at 4°C for 30 minutes. After washing with PBS to remove unbound antibodies, cells were analyzed by a BD FACSCalibur flow cytometer (BD Biosciences, San Jose, CA, USA). Flow cytometry data analysis was performed using Flowing Software version 2.

2.3 Generation of fibrin gel

Fibrin gel preparation and selection of ingredient concentrations were performed as described in our previous study (18). Briefly, PB samples were collected from three volunteers using EDTA as the anticoagulant. Plasma fractions were separated by centrifugation at 1500 rpm for 5 minutes and pooled. Plasma samples were stored at -20°C. Fibrin gels were generated using 40 µl of thawed plasma samples, 1 mg/ml calcium chloride (Cat# C7902, Sigma-Aldrich, Darmstadt, Germany) and 5 mg/ml tranexamic acid (Caspian Tamin Pharma. Co., Rasht, Iran) in a total volume of 100 µl in RPMI-1640 media.

2.4 Generation of 3D cell structures

U266, BM-MSCs and HUVECs were co-cultured under three different conditions: 1) in non-adherent culture plates without any matrices (stated as the gel-free group), 2) in fibrin gel-coated plates (referred to as the on-gel group), and 3) inside fibrin gels (stated as the inside-gel group) (Figure 1). In all experimental groups, 3×10^4 U266 cells, 10^4 BM-MSCs and 10^4 HUVECs (3:1:1 ratio) were mixed in the 100 µl total volume of RPMI1640 complete culture media or fibrin gel mixture (19). In the gel-free group, the cell mixtures were co-cultured in 96-well non-adherent culture plates to prevent cell attachment to the culture surface, enabling aggregation and 3D structure formation in the absence of an external extracellular

matrix, and were force-aggregated by centrifugation at 200 g for 5 minutes at 22°C (20). In the on-gel group, fibrin gels were added to culture plates, and after gelation, the cell mixtures were cultured on fibrin matrices. Low-attachment plates were not used in this condition. In the inside-gel group, cells were suspended in complete culture media mixed with plasma, and then, calcium chloride and tranexamic acid were added to initiate gelation. Then, each 100 µl of cell/gel mixture was placed in non-adherent culture plates as droplet-like structures, and culture media were added when gels were formed (18). Non-adherent plates were used in this group to prevent cells from migrating out of the gel and adhering to the plate surface, and to facilitate handling of the fibrin constructs during downstream analyses. The medium was changed every three days in all experimental groups. Cell proliferation and viability assessments were performed on days 3 and 7 post co-culture.

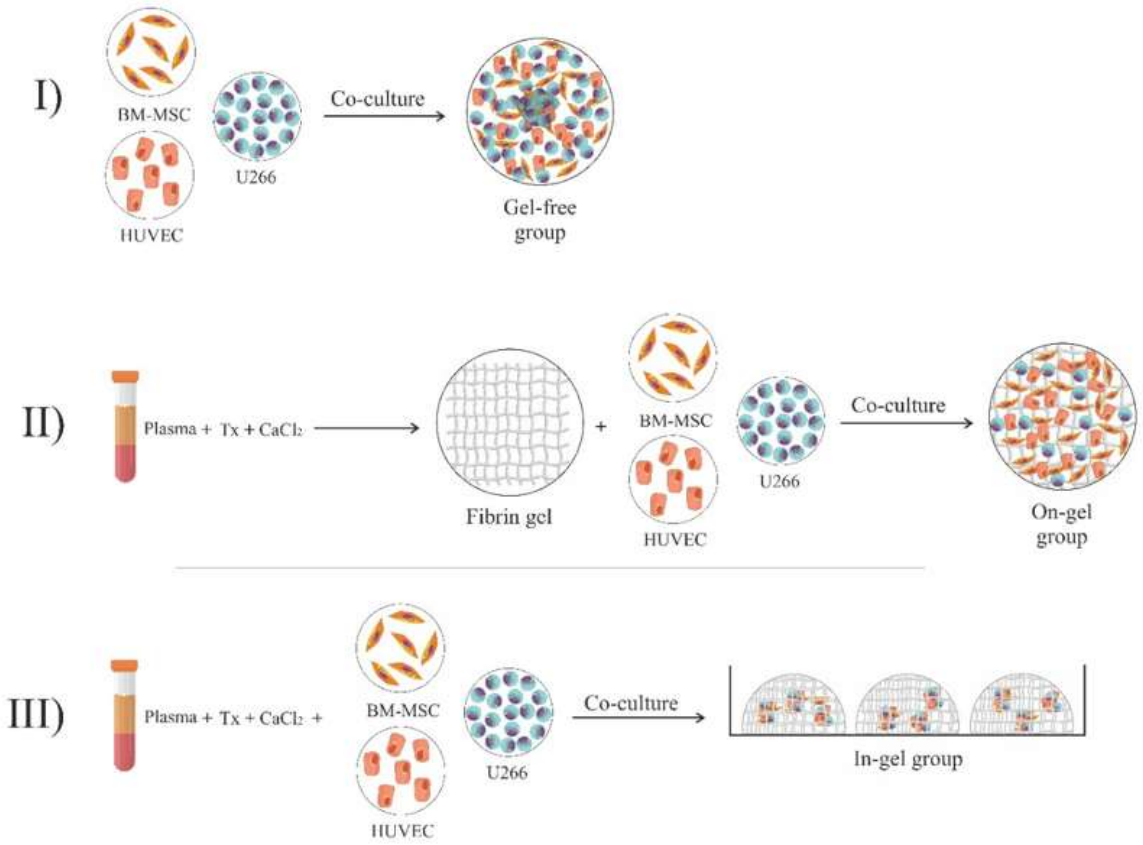

Figure 1. Schematic illustration of the study design. U266 cells were co-cultured with BM-MSCs and HUVECs under gel-free and matrix-based conditions to develop a simple and cost-effective three-dimensional (3D) co-culture model. Tx: tranexamic acid (**Prepared by Authors, 2026**).

2.5 Cell proliferation and viability assessment

Gel-free cell structures were incubated and digested using trypsin-EDTA 0.025% at 37°C for 2 minutes. The generated droplet-like cell/gel structures were washed and digested in 5 mg/ml collagenase type I (Cat# 17100-017, Gibco, USA) enzyme at 37°C (18). After complete digestion of the gels, the enzyme was diluted with culture medium and removed by centrifugation at 1500 rpm for 5 minutes. Cell proliferation was measured using the trypan blue staining method (Cat# BI-1803, Bioidea, Tehran, Iran) on days 3 and 7 post co-culture. Cells without color were considered to be live cells.Cell expansion fold was calculated as the ratio of counted live cells to the cell seeding count (5×10^4 cells). Moreover, the viability of U266 cells was measured three and seven days after co-culture by propidium-iodide (PI; Cat# P4170, Sigma-Aldrich, Darmstadt, Germany) and anti-CD138 double staining using the flow cytometry technique.

For this purpose, washed cells were incubated with FITC-conjugated CD138 antibody at 4°C for 30 minutes. Thereafter, cells were washed to remove unbound antibodies and were stained with 1 mg/ml PI. Cells were analyzed by a BD FACSCalibur flow cytometer.

2.6 Statistical analysis

Experiments were performed with at least three independent replications. Data is presented as mean ± standard deviation. The significant differences between groups were analyzed by student's t-test and ANOVA (Tukey's post-hoc test) using GraphPad Prism software. The differences were considered statistically significant with $P<0.05$.

3. Result

3.1 Development of co-culture conditions

To generate *in vitro* structures more closely resembling the myeloma microenvironment for further studies, U266 cells were co-cultured with BM-MSCs and HUVECs. As shown in Figure 2a-b, BM-MSCs had spindle-shape morphology and expressed CD90 and CD105 surface markers. Moreover, Oil Red O and Alizarin Red staining revealed the adipogenic and osteogenic differentiation potential of BM-MSCs (Figure 2 c). HUVECs showed cobblestone-like morphology and expressed the CD31 surface marker (Figure 2 d-e).

Co-culture of U266 cells, BM-MSCs, and HUVECs was carried out in different matrix-based and matrix-free culture conditions. Figure 3 shows the morphology of co-cultured cells in gel-free, on-gel and inside-gel conditions over a seven-day period. Cells in the gel-free group could generate 3D cell structures one day after co-culture, and the formed structures became condensed over the culture period (Figure 3 a). However, the organization of co-cultured cells into 3D structures was not observed in the on-gel group (Figure 3 b).

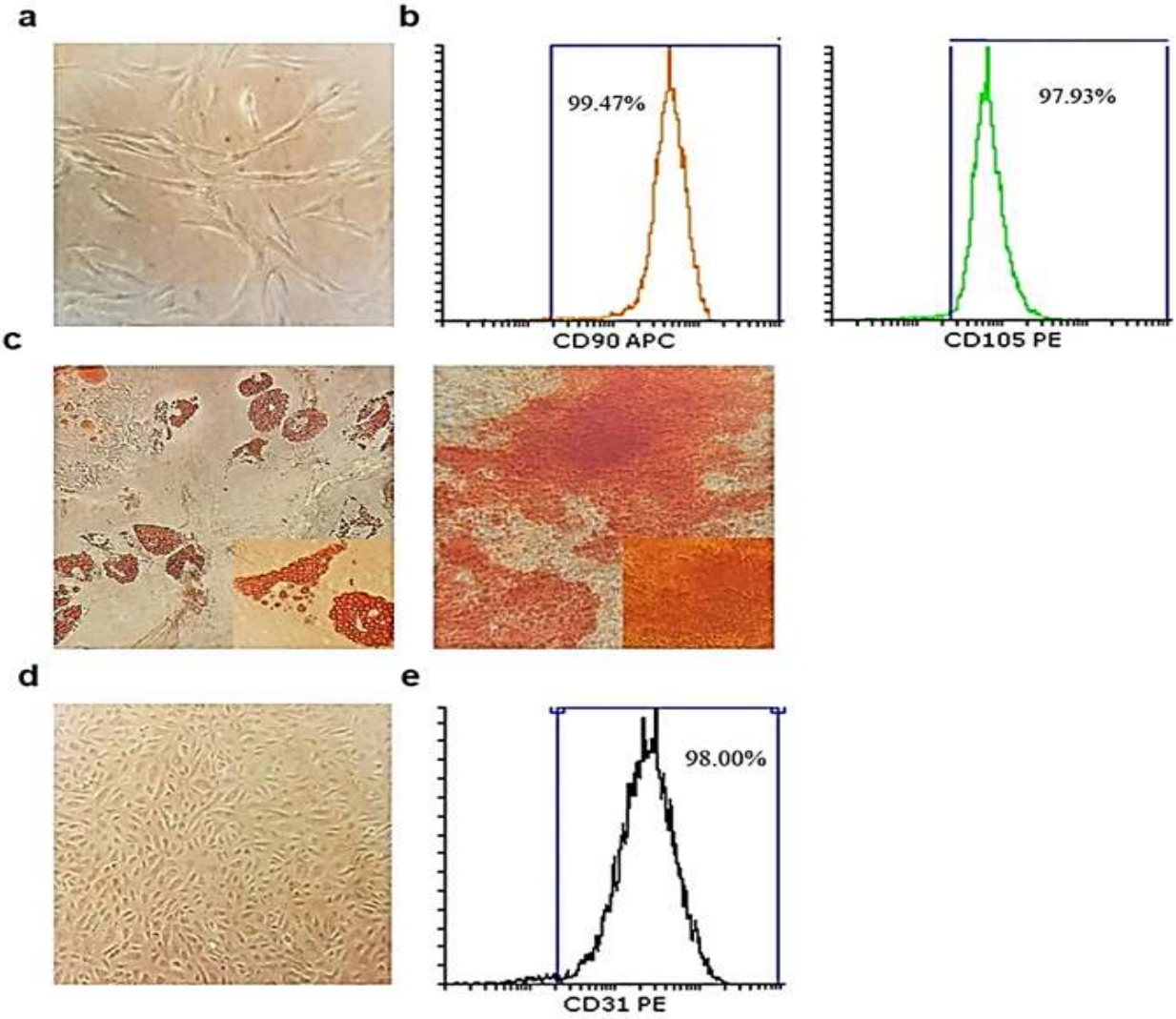

Figure 2. BM-MSCs and HUVECs culture and flow cytometry analysis. a) Phase-contrast image of BM-MSCs (×20), b) Flow cytometry analysis of BM-MSCs for CD90 and CD105 expression, c) Differentiation potential of BM-MSC into adipocytes and osteoblasts assessed by Oil Red O and Alizarin Red staining, respectively (×20), d) Phase-contrast image of HUVECs (×20), e) Flow cytometry analysis of HUVECs for CD31 expression. (**Prepared by Authors, 2026**).

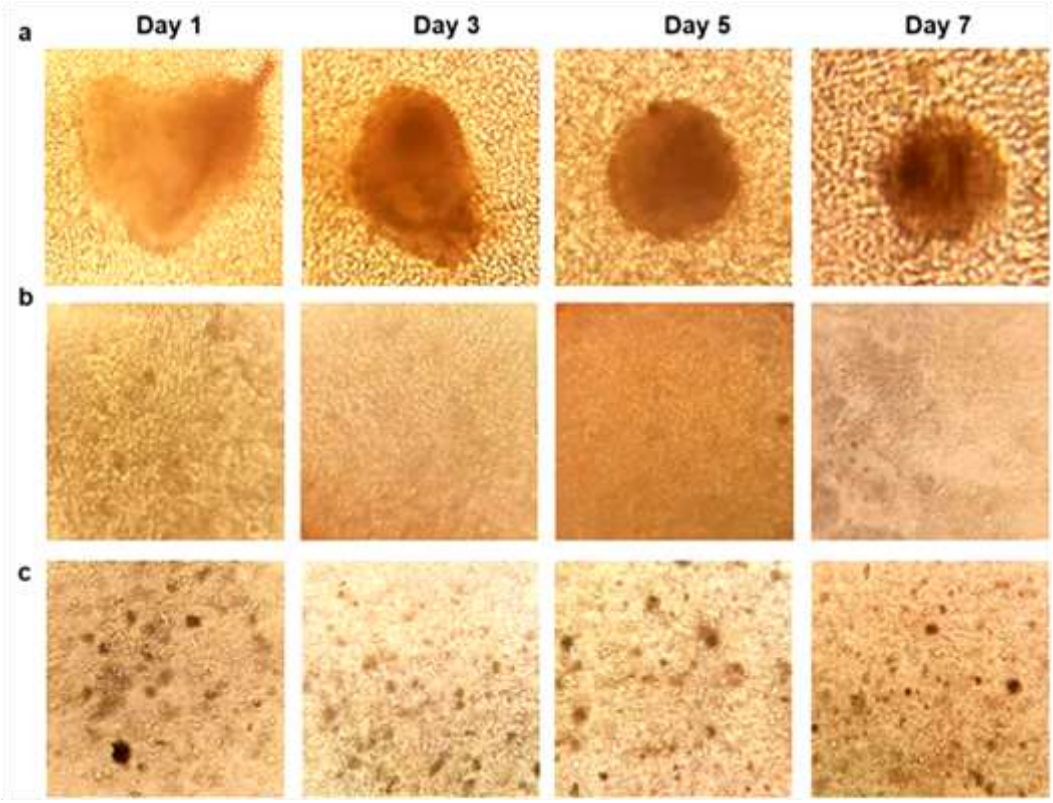

Figure 3. Phase-contrast images of co-cultured U266 cells, BM-MSCs and HUVECs at days 1, 3, 5 and 7 after co-culture in a) gel-free (×10), b) on-gel (×10), and c) inside-gel groups (×10). (**Prepared by Authors, 2026**).

3.2 The survival rate of U266 cells in co-culture conditions

Flow cytometry analysis of co-cultured cells at day three showed that 80.9 ± 6.8%, 47.1 ± 8.1%, and 12.7 ± 5.1% of cells were positive for the CD138 marker in gel-free, on-gel and inside-gel groups, respectively (Figure 4a). The percentage of $CD138^+$ cells in the gel-free group was significantly higher than those of the on-gel and inside-gel groups. Moreover, as presented in Figure 4a, the percentage of $CD138^+$ cells at day three of culture in the inside-gel group was significantly less than two other groups. Seven days after co-culture, the percentages of CD138 positive cells decreased to 74.2 ± 11.4%, 34.6 ± 21.5%, and 7.6 ± 2.6% although the differences between days three and seven of each group were not statistically significant (Figure 4a). Similar to day three, the percentage of $CD138^+$ cells in the gel-free group at day seven after co-culture was significantly higher than those of the on-gel and inside-gel groups (Figure 4a).

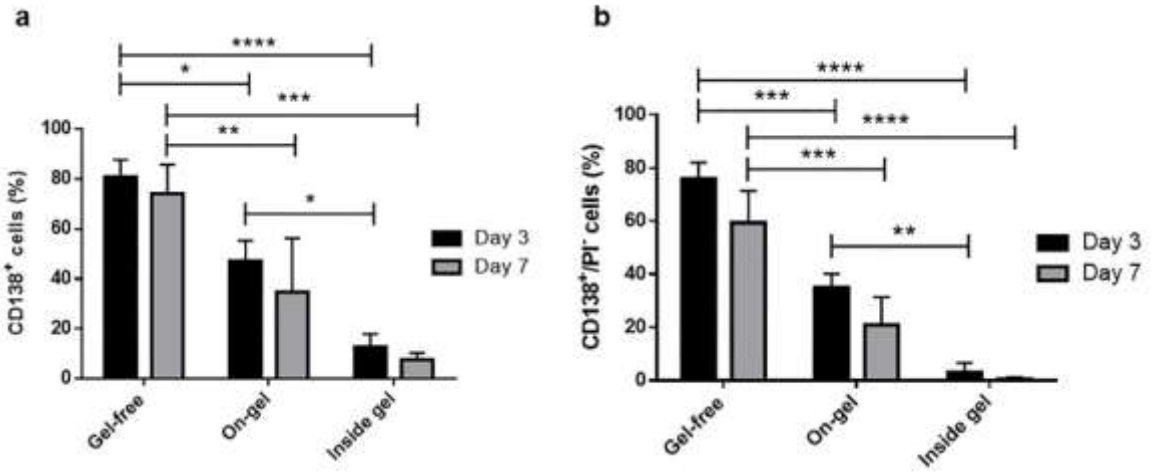

Figure 4. Flow cytometry analysis of co-cultured cells at days three and seven. a) The percentage of $CD138^+$ cells in three different co-culture groups, b) The percentage of $CD138^+/PI^-$cells in three different co-culture groups. The data is presented as mean ± standard deviation, *: $P \leq 0.05$, **: $P \leq 0.01$, ***: $P \leq 0.001$ and ****: $P \leq 0.0001$. (**Prepared by Authors, 2026**).

On the other hand, flow cytometry of CD138/PI double-stained co-cultured cells at day three revealed that 75.9 ± 6%, 35 ± 5.1%, and 3 ± 3.6% of cells were $CD138^+/PI^-$ in gel-free, on-gel and inside-gel groups, respectively (Figure 4b). The percentage of $CD138^+/PI^-$ cells at day three in the gel-free group was significantly higher than those of the gel-free and on-gel groups.
As it is presented in Figure 4b, seven days after co-culture, 61.5 ± 15.7%, 20.9 ± 10.5%, and 0.5 ± 0.5% of cells were $CD138^+/PI^-$ in gel-free, on-gel and inside-gel groups, respectively. Similar to day three, the viability of $CD138^+$ cells in the gel-free group was significantly higher than the other two groups, at day seven (Figure 4b).

3.3 The proliferation rate of U266 cells in co-culture conditions

The expansion fold measurement showed that co-cultured cells at day three of culture in the gel-free group proliferated 1.5 ± 0.3 times more than the seeding count (Figure 5a). At day seven, the expansion fold of co-cultured cells in the gel-free group was increased to 4 ± 0.8. However, as presented in Figure 5a, the calculated expansion folds of cells in the on-gel group were 0.9 ± 0.2 and 0.6 ± 0.4 at days three and seven after co-culture, respectively. Moreover, the pattern of increase in expansion folds over seven days (0.8 ± 0.5 at day three and 2.4 ± 1.9 at day seven) was observed in the inside-gel group, similar to the gel-free group (Figure 5a). Statistical analysis revealed that the calculated expansion fold of cells in the on-gel group at day seven of culture was significantly less than that of the gel-free group.

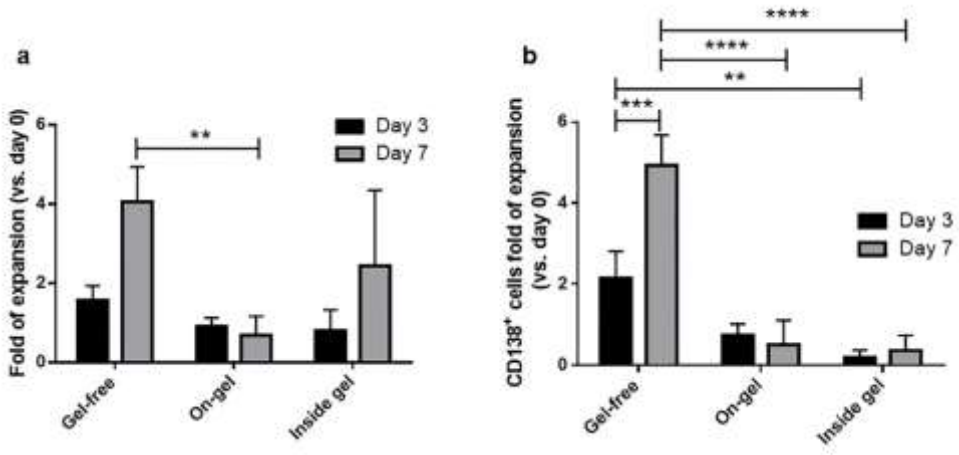

Figure 5. Calculated expansion folds of co-cultured cells at days three and seven versus day zero. a) Expansion folds of cells in three different co-culture groups, b) Expansion folds of $CD138^+$cells in three different co-culture groups. The data is presented as mean ± standard deviation, **: P ≤ 0.01, ***: P ≤ 0.001 and ****: P ≤ 0.0001.

As presented in Figure 5b, at day three of co-culture, the calculated expansion folds of $CD138^+$ cells were 2.1 ± 0.6, 0.7 ± 0.2 and 0.1± 0.1 times the seeding counts in gel-free, on-gel and inside-gel groups, respectively. The expansion fold of $CD138^+$ cells at day three in the gel-free group was significantly higher than that of the inside-gel group. Moreover, expansion folds of $CD138^+$ cells in the on-gel and inside-gel groups at day seven of co-culture were significantly less than those of the gel-free group.

4. Discussion

Fabrication of tissue-like structures to mimic 3D cell-cell and cell-ECM interactions present in native tissues is both challenging and promising in disease modeling and drug screening studies (21). In the case of MM, various BM-mimicking constructs have been developed as *in vitro* tools for disease study and drug testing (22).Notably, sources of patient-dependent primary cells are relatively limited. Moreover, primary cells without suitable microenvironmental supports in the culture conditions are maintained for a limited time (23). Therefore, in this study, an attempt was made to generate simple and patient-independent co-culture-based 3D structures in order to produce myeloma tissue-like cell cultures. In this regard, the U266 myeloma cell line was co-cultured with BM-MSCs and HUVECs in different matrix-free and matrix-based culture conditions, which were further analyzed and compared in terms of U266 cell viability and proliferation rates.
It has been confirmed that malignant myeloma cells, and their microenvironment, are directly or indirectly affected by distinct cell types (24). MSCs and endothelial cells are important cells in the BM that influence the proliferation, survival and drug resistance of myeloma cells. Activation of the Notch signaling pathway in both MM cells and BM stromal cells induces secretion of IL-6, VEGF and IGF-1 and is associated with myeloma cell proliferation and survival (25). Although it has been shown that gene expression and cytokine secretion of patient-derived BM-MSCs differ from those of normal BM-MSCs (26), co-culture of normal BM-MSCs with myeloma cells could alter the gene expression patterns and signaling pathways of normal MSCs to become similar to patient-derived cells (27). It is well-established that angiogenesis is

important for MM growth and metastasis. MM cells secrete VEGF, which triggers endothelial cells to secrete IL-6; this dynamic crosstalk determines the proliferation of both MM cells and endothelial cells (28). According to the importance and impact of MSCs and endothelial cells on myeloma cell features and responses, similar studies co-cultured myeloma cell lines or primary cells with MSCs and endothelial cells to recapitulate the disease microenvironment (29, 30).

To generate 3D cell structures, three different culture conditions were used and compared. In our first group, cells were co-cultured without a matrix and force-aggregated to from 3D structures. It has been shown that the existence of stromal cells in co-cultures could promote and enhance this assembly (31). For instance, Djomehri et al. co-cultured breast cancer cell lines and MSCs in scaffold-free conditions and observed the formation of 3D structures after three days of culture (32). In our second co-culture group, cells were cultured on a fibrin gel-based coating. Similar studies have used a variety of ECM coatings, including Matrigel, to enhance the self-organization of cultured cells (33, 34). However, we did not observe the generation of cell clusters over 7 days of co-culture on fibrin gels. This may be attributed to the type of coated matrix used in our study compared with Matrigel (35). In the third group, cells were cultured inside the fibrin gel. Fibrin gels have been widely used as 3D scaffolds for generating of tissue and organ-like structures to study various diseases, including chronic lymphocytic leukemia, acute myelogenous leukemia, and chronic myelogenous leukemia (13). Previous studies mostly used BM aspirate to fabricate fibrin gel-based structures; however, we tried to generate available fibrin gels by using PB plasma. Despite differences in the cytokine content, it has been shown that the fibrinogen levels of PB and BM samples did not significantly differ (36). It should be emphasized that using PB plasma samples rather than MM patient-derived BM plasma may have affected the proliferation and survival of U266 cells in our study. Notably, in our previous study, we successfully generated a PB-derived fibrin gel-based 3D mono-culture system for U266 cells and demonstrated that this structure could support myeloma cell viability and proliferation under optimized conditions (18). However, in the present study, two additional cellular components, BM-MSCs and endothelial cells, were introduced into the culture systems. Moreover, in recent years, more complex 3D structures, such as microgel-based systems, have been developed, that can successfully maintain the viability and proliferation of myeloma cells (37). In contrast, we intentionally employed simple and accessible strategies to culture myeloma cells with BM-MSCs and endothelial cells.

The percentage of $CD138^+$ cells in the gel-free group was significantly higher compared to the other groups. Consistent with our study, de la Puente and colleagues reported higher percentages of CD138 expression in the gel-free group compared to the inside-gel group (19). Moreover, the viability and expansion fold of U266 cells in the gel-free group were significantly higher compared to those in the on-gel and inside gel groups. However, other studies reported the increased viability and proliferation of myeloma cells when co-cultured with MSCs and endothelial cells in Matrigel and BM-derived fibrin gel (19, 29, 30). It has been demonstrated that the proliferation rate of MSCs co-cultured with HUVECs in fibrin gels was significantly higher compared to the mono-culture of MSCs in the 2D culture condition (38). Accordingly, the significantly lower levels of proliferation rate and viability of CD138 positive cells in on-gel and inside-gel groups compared to the gel-free group may be attributed to the dominant proliferation of MSCs and HUVECs in these conditions, which prevented the proliferation and survival of MM cells; however, this hypothesis requires evaluation and confirmation in future studies. In this regard, tracking lineage-specific markers in BM-MSCs and HUVECs or using multiplex imaging strategies can help determine the fate and distribution of each cell type, thereby achieving a more comprehensive characterization of 3D co-culture systems. On the other hand, more precise evaluation and tracking of U266 cells in 3D cultures require histological assessments; therefore, the observed decrease of viable cells may be attributed to the enzymatic digestion of structures for the flow cytometry analysis and the usage of non-destructive techniques, including the application of cell tracking dyes, may help reduce the potential negative influence of enzymatic processing. Moreover, assessing IL-6 secretion is highly recommended in future studies to indicate the functionality of cultured MM cells.

5. Conclusion

In this study, we tried to generate a simple, cost-beneficial, patient-independent and available 3D co-culture condition for U266 MM cells with MSCs and endothelial cells. Our different matrix-based and matrix-free culture conditions showed significantly higher survival and proliferation rates of CD138 positive cells in gel-free cultures. This gel-free culture condition can be suggested as a suitable platform for further *in vitro* studies, including drug screening.

6. Declarations

6.1 Acknowledgments

The authors would like to thank the peripheral blood donors.

6.2 Ethical Considerations

This study was performed in accordance with the Ethics Committee of Tarbiat Modares University (code: IR.MODARES.REC.1399.229).

6.3 Authors' Contributions

MK: study design, data analysis, data presentation and draft preparation; SV: study supervision, project administration, editing and finalizing the manuscript; SA: study consultation, editing and finalizing the manuscript. All authors have approved the final version of the manuscript.

6.4 Conflict of Interest

The authors have no competing interests to declare that are relevant to the content of this article.

6.5 Fund or Financial Support

The research leading to these results received funding from Tarbiat Modares University and a grant from the Iran National Science Foundation (INSF) to Sadaf Vahdat under Grant Agreement No. 99024778.

6.6 Using Artificial Intelligence Tools (AI Tools)

The authors were not utilized AI Tools for data generation, data analysis, and manuscript preparation.

References

1. Malard F, Neri P, Bahlis NJ, Terpos E, Moukalled N, Hungria VTM, et al. Multiple myeloma. Nat Rev Dis Primers. 2024;10(1):45. [DOI:10.1038/s41572-024-00529-7] [PMID]

2. Mondello P, Cuzzocrea S, Navarra M, Mian M. Bone marrow micro-environment is a crucial player for myelomagenesis and disease progression. Oncotarget. 2017;8(12):20394. [DOI:10.18632/oncotarget.14610] [PMID] [PMCID]

3. Papadimitriou K, Kostopoulos IV, Tsopanidou A, Orologas-Stavrou N, Kastritis E, Tsitsilonis O, et al. Ex vivo models simulating the bone marrow environment and predicting response to therapy in multiple myeloma. Cancers (Basel). 2020;12(8):2006. [DOI:10.3390/cancers12082006] [PMID] [PMCID]

4. Ho M, Goh CY, Patel A, Staunton S, O'Connor R, Godeau M, et al. Role of the bone marrow milieu in multiple myeloma progression and therapeutic resistance. Clin Lymphoma Myeloma Leuk. 2020;20(10):e752-e68. [DOI:10.1016/j.clml.2020.05.026] [PMID]

5. Teramachi J, Miki H, Nakamura S, Hiasa M, Harada T, Abe M. Myeloma bone disease: pathogenesis and management in the era of new anti-myeloma agents. J Bone Mineral Metab. 2023;41(3):388-403. [DOI:10.1007/s00774-023-01403-4] [PMID] [PMCID]

6. Ribatti D, Vacca A. New insights in anti-angiogenesis in multiple myeloma. Int J Molec Sci. 2018;19(7):2031. [DOI:10.3390/ijms19072031] [PMID] [PMCID]

7. Giannakoulas N, Ntanasis-Stathopoulos I, Terpos E. The role of marrow microenvironment in the growth and development of malignant plasma cells in multiple myeloma. Int J Molec Sci. 2021;22(9):4462. [DOI:10.3390/ijms22094462] [PMID] [PMCID]

8. Martini S, Drzeniek NM, Stark R, Kollert MR, Du W, Reinke S, et al. Long-term in vitro maintenance of plasma cells in a hydrogel-enclosed human bone marrow microphysiological 3D model system. Biofabrication. 2024;16(4):045005. [DOI:10.1088/1758-5090/ad5dfe] [PMID]

9. Mehdi SH, Nafees S, Mehdi SJ, Morris CA, Mashouri L, Yoon D. Animal models of multiple myeloma bone disease. Front Genet. 2021;12:640954. [DOI:10.3389/fgene.2021.640954] [PMID] [PMCID]

10. Ferrarini M, Marcatti M, Ciceri F, Ferrero E. 3D Models of surrogate multiple myeloma bone marrow microenvironments: Insights on disease pathophysiology and patient-specific response to drugs. Multiple Myeloma. 2021:93. [DOI:10.5772/intechopen.95333]

11. Verbruggen SW, Freeman CL, Freeman FE. Utilizing 3D models to unravel the dynamics of myeloma plasma cells' escape from the bone marrow microenvironment. Cancers. 2024;16(5):889. [DOI:10.3390/cancers16050889] [PMID] [PMCID]

12. Calar K, Plesselova S, Bhattacharya S, Jorgensen M, de la Puente P. Human plasma-derived 3D cultures model breast cancer treatment responses and predict clinically effective drug treatment concentrations. Cancers (Basel). 2020;12(7):1722. [DOI:10.3390/cancers12071722] [PMID] [PMCID]

13. Alhallak K, de la Puente P, Jeske A, Sun J, Muz B, Rettig MP, et al. 3D tissue engineered plasma cultures support leukemic proliferation and induces drug resistance. Leuk Lymphoma. 2021;62(10):2457-65. [DOI:10.1080/10428194.2021.1919657] [PMID]

14. Barbosa MA, Xavier CP, Pereira RF, Petrikaitė V, Vasconcelos MH. 3D cell culture models as recapitulators of the tumor microenvironment for the screening of anti-cancer drugs. Cancers. 2022;14(1):190. [DOI:10.3390/cancers14010190] [PMID] [PMCID]

15. Ferreira L, Gaspar V, Mano J. Design of spherically structured 3D in vitro tumor models-advances and prospects. Acta Biomaterialia. 2018;75:11-34. [DOI:10.1016/j.actbio.2018.05.034] [PMID] [PMCID]

16. Zlei M, Egert S, Wider D, Ihorst G, Wasch R, Engelhardt M. Characterization of in vitro growth of multiple myeloma cells. Exp Hematol. 2007;35(10):1550-61. [DOI:10.1016/j.exphem.2007.06.016] [PMID]

17. Kaur G, Dufour JM. Cell lines: Valuable tools or useless artifacts. Taylor & Francis; 2012. p. 1-5. [DOI:10.4161/spmg.19885] [PMID] [PMCID]

18. Jomehpour M, Khosravi M, Janfada M, Abroun S, Vahdat S. Establishment of a three-dimensional culture condition for the U266 cell line based on peripheral blood plasma-derived fibrin gels. Cell J (Yakhteh). 2023;25(4):229.

19. de la Puente P, Muz B, Gilson RC, Azab F, Luderer M, King J, et al. 3D tissue-engineered bone marrow as a novel model to study pathophysiology and drug resistance in multiple myeloma. Biomaterials. 2015;73:70-84. [DOI:10.1016/j.biomaterials.2015.09.017] [PMID] [PMCID]

20. Xie AW, Binder BYK, Khalil AS, Schmitt SK, Johnson HJ, Zacharias NA, et al. Controlled self-assembly of stem cell aggregates instructs pluripotency and lineage bias. Sci Rep. 2017;7(1):14070. [DOI:10.1038/s41598-017-14325-9] [PMID] [PMCID]

21. de Janon A, Mantalaris A, Panoskaltsis N. Three-dimensional human bone marrow organoids for the study and application of normal and abnormal hematoimmunopoiesis. J Immunol. 2023;210(7):895-904. [DOI:10.4049/jimmunol.2200836] [PMID] [PMCID]

22. Garcia-Ortiz A, Rodriguez-Garcia Y, Encinas J, Maroto-Martin E, Castellano E, Teixido J, et al. The role of tumor microenvironment in multiple myeloma development and progression. Cancers. 2021;13(2). [DOI:10.3390/cancers13020217] [PMID] [PMCID]

23. Huang YH, Almowaled M, Li J, Venner C, Sandhu I, Peters A, et al. Three-dimensional reconstructed bone marrow matrix culture improves the viability of primary myeloma cells in-vitro via a STAT3-dependent mechanism. Curr Issues Mol Biol. 2021;43(1):313-23. [DOI:10.3390/cimb43010026] [PMID] [PMCID]

24. Garcia-Ortiz A, Rodríguez-García Y, Encinas J, Maroto-Martín E, Castellano E, Teixidó J, et al. The role of tumor microenvironment in multiple myeloma development and progression. Cancers. 2021;13(2):217. [DOI:10.3390/cancers13020217] [PMID] [PMCID]

25. Lu K, Wang W, Liu Y, Xie C, Liu J, Xing L. Advancements in microenvironment-based therapies: transforming the landscape of multiple myeloma treatment. Front Oncol. 2024;14:1413494. [DOI:10.3389/fonc.2024.1413494] [PMID] [PMCID]

26. Garayoa M, Garcia JL, Santamaría C, García-Gómez A, Blanco JF, Pandiella A, et al. Mesenchymal stem cells from multiple myeloma patients display distinct genomic profile as compared with those from normal donors. Leukemia. 2009;23(8):1515-27. [DOI:10.1038/leu.2009.65] [PMID]

27. Attar-Schneider O, Zismanov V, Dabbah M, Tartakover-Matalon S, Drucker L, Lishner M. Multiple myeloma and bone marrow mesenchymal stem cells' crosstalk: Effect on translation initiation. Molec Carcinogen. 2016;55(9):1343-54. [DOI:10.1002/mc.22378] [PMID]

28. Melaccio A, Reale A, Saltarella I, Desantis V, Lamanuzzi A, Cicco S, et al. Pathways of angiogenic and inflammatory cytokines in multiple myeloma: role in plasma cell clonal expansion and drug resistance. J Clin Med. 2022;11(21):6491. [DOI:10.3390/jcm11216491] [PMID] [PMCID]

29. Belloni D, Heltai S, Ponzoni M, Villa A, Vergani B, Pecciarini L, et al. Modeling multiple myeloma-bone marrow interactions and response to drugs in a 3D surrogate microenvironment. Haematologica. 2018;103(4):707-16. [DOI:10.3324/haematol.2017.167486] [PMID] [PMCID]

30. Braham MVJ, Minnema MC, Aarts T, Sebestyen Z, Straetemans T, Vyborova A, et al. Cellular immunotherapy on primary multiple myeloma expanded in a 3D bone marrow niche model. Oncoimmunol. 2018;7(6):e1434465. [DOI:10.1080/2162402X.2018.1434465] [PMID] [PMCID]

31. Takebe T, Enomura M, Yoshizawa E, Kimura M, Koike H, Ueno Y, et al. Vascularized and complex organ buds from diverse tissues via mesenchymal cell-driven condensation. Cell Stem Cell. 2015;16(5):556-65. [DOI:10.1016/j.stem.2015.03.004] [PMID]

32. Djomehri SI, Burman B, Gonzalez ME, Takayama S, Kleer CG. A reproducible scaffold-free 3D organoid model to study neoplastic progression in breast cancer. J Cell Commun Signal. 2019;13(1):129-43. [DOI:10.1007/s12079-018-0498-7] [PMID] [PMCID]

33. Varzideh F, Pahlavan S, Ansari H, Halvaei M, Kostin S, Feiz MS, et al. Human cardiomyocytes undergo enhanced maturation in embryonic stem cell-derived organoid transplants. Biomaterials. 2019;192:537-50. [DOI:10.1016/j.biomaterials.2018.11.033] [PMID]

34. Takebe T, Zhang RR, Koike H, Kimura M, Yoshizawa E, Enomura M, et al. Generation of a vascularized and functional human liver from an iPSC-derived organ bud transplant. Nat Protoc. 2014;9(2):396-409. [DOI:10.1038/nprot.2014.020] [PMID]

35. Li Y, Meng H, Liu Y, Lee BP. Fibrin gel as an injectable biodegradable scaffold and cell carrier for

tissue engineering. Sci W J. 2015;2015. [DOI:10.1155/2015/685690] [PMID] [PMCID]

36. Shoji T, Nakasa T, Yoshizuka M, Yamasaki T, Yasunaga Y, Adachi N, et al. Comparison of fibrin clots derived from peripheral blood and bone marrow. Connect Tissue Res. 2017;58(2):208-14. [DOI:10.1080/03008207.2016.1215443] [PMID]

37. Garcia-Briega MI, Pla-Salom J, Clara-Trujillo S, Tolosa L, Cordon L, Sempere A, et al. Co-culture of multiple myeloma cell lines and bone marrow mesenchymal stem cells in a 3D microgel environment. Biomaterials advances. 2025;172:214243.

[DOI:10.1016/j.bioadv.2025.214243] [PMID]

38. Heo DN, Hospodiuk M, Ozbolat IT. Synergistic interplay between human MSCs and HUVECs in 3D spheroids laden in collagen/fibrin hydrogels for bone tissue engineering. Acta biomaterialia. 2019;95:348-56.[DOI:10.1016/j.actbio.2019.02.046] [PMID]